The rotational spectrum, structure, and molecular properties of the ethylene–HCl dimer

P. D. Aldrich, A. C. Legon, and W. H. Flygare

Citation: The Journal of Chemical Physics **75**, 2126 (1981); doi: 10.1063/1.442316
View online: http://dx.doi.org/10.1063/1.442316
View Table of Contents: http://scitation.aip.org/content/aip/journal/jcp/75/5?ver=pdfcov
Published by the AIP Publishing

The rotational spectrum, structure, and molecular properties of the ethylene–HCl dimer

P. D. Aldrich, A. C. Legon, and W. H. Flygare[a)]

Noyes Chemical Laboratory, University of Illinois, Urbana, Illinois 61801
(Received 23 April 1981; accepted 22 May 1981)

Three isotopic species of a hydrogen bonded dimer formed between ethylene and HCl have been observed through assignment of their rotational spectra using a pulsed, Fourier transform microwave spectrometer in which a gas mixture is pulsed into an evacuated Fabry–Perot cavity. The spectra unambiguously reveal a nonplanar, near prolate, asymmetric top ($\kappa = -0.9880$) in its ground vibrational state. The equilibrium structure has C_{2v} symmetry with the HCl on the C_2 symmetry axis of the dimer, perpendicular to the carbon–carbon bonding axis with the hydrogen atom located between the chlorine and the ethylene molecule, pointing midway between the carbon atoms. The chlorine atom is situated, on average, 3.724 Å from the edge of the ethylene molecule. The following spectroscopic constants have been obtained for the ethylene–$H^{35}Cl$ dimer: the rotational constants are $A = 25\,457(349)$, $B = 2308.143(3)$, and $C = 2167.970(3)$ in units of MHz; the chlorine nucleus quadrupole coupling constants are $\chi_{aa} = -54.076(4)$, $\chi_{bb} = 27.091(6)$, and $\chi_{cc} = 26.985(10)$ in units of MHz, and the centrifugal distortion constants are $D_J = 7.2(2)$ and $D_{JK} = 282(5)$ in units of kHz.

INTRODUCTION

We have recently been involved in the identification and characterization of a number of hydrogen-bound dimers formed between HCl and organic molecules through assignment of their rotational spectra. We have previously reported on the discovery of both the cyclopropane–HCl and the acetylene–HCl dimers and have characterized them as similar in binding strength and internal dynamics to other hydrogen-bound dimers.[1–3] The present dimer, ethylene–HCl, is, however, especially interesting because of the question of planarity versus nonplanarity. It is with the resolution of this question that we now report the observation and subsequent assignment of the rotational spectrum of the ethylene–HCl dimer using a pulsed, Fourier transform microwave spectrometer where the microwaves and the gas mixture are simultaneously pulsed into an evacuated Fabry–Perot cavity. Interpretation of the spectrum reveals a nonplanar asymmetric top ($\kappa = -0.9880$) in its ground vibrational state with C_{2v} symmetry for its equilibrium structure. The HCl lies, on average, on the C_2 axis of symmetry with the hydrogen atom situated between the chlorine atom and ethylene's carbon–carbon axis and pointing towards the middle of the ethylene double bond. Analysis of the spectrum further points to the dimer being a hydrogen-bound complex with the attractive interaction being between the electrophilic hydrogen on the hydrogen halide and the π electron density of the ethylene. This is in contrast to the looser bound, more traditional van der Waals complexes formed between rare gases and hydrogen halides.

The existence of the dimer is not surprising, especially in view of the recent discovery of the acetylene–HCl dimer. However, the existence of weakly bound π complexes has been postulated before as occurring as reactive intermediates in the addition reactions of unsaturated hydrocarbons.[4–6] Intuition leads one to envision an intermediate which includes a nucleophilic unsaturated hydrocarbon and, in the case of addition reactions with hydrogen halides, an electrophilic hydrogen on the hydrogen halide. Much insight into the nature of such dimers is available from their rotational spectra which, when obtained at low pressures and high resolution, allow properties of the isolated dimer, and hence the weak binding, to be investigated in the absence of lattice or solvent effects. Our present spectrometer is well suited to the observation of high resolution spectra for species that, like the present dimer, exist in very low number density under normal temperature and pressure conditions.

EXPERIMENTAL

The ethylene–HCl dimers were generated by expanding a gas mixture consisting of 2% of both HCl and ethylene in argon, and initially at room temperature and 0.5–2.5 atm, through a 0.5 mm diameter pulsed supersonic nozzle into a vacuum of $\sim 10^{-5}$ Torr. The vibrational, rotational, and translational temperatures are consequently cooled to 1–10 K. All rotational transitions within the cavity bandwidth (~1 MHz) were then polarized by a suitably delayed 3.0 μs microwave power pulse. The spectrometer which has been described previously in detail[7–9] was next used to record the time domain emission signal which is subsequently digitized at a rate of 0.5 μs per point for 256 points. Approximately 20 signals are then averaged with gas in the cavity and subtracted from an equal average with no gas present in order to eliminate any coherent noise. The averaged signal is then Fourier transformed to give the power spectrum which consists of 256 points at 3.9 kHz per point resolution. A characteristic Doppler doubling is present in the frequency spectrum with the actual molecular resonance located at the midpoint of the two Doppler components. This phenomenon is well understood and has been described in detail elsewhere.[10] The half widths at half height are typically ~5 kHz with the frequency uncertainty being ~3 kHz.

Three $\mu_a R$ branches were observed between 4 and 14 GHz for the ethylene–$H^{35}Cl$ and ethylene–$H^{37}Cl$ isotopes. Two R branches were observed for the ethylene–$D^{35}Cl$ isotope.

[a)]Deceased.

 0021-9606/81/172126-09$01.00

TABLE I. Observed and calculated transition frequencies for C_2H_4–$H^{35}Cl$ (experimental uncertainty is estimated to be 3 kHz).

Rotational transition	$F \rightarrow F'$	Observed (MHz)	Calculated (MHz)	Difference (kHz)
$0_{00} \rightarrow 1_{01}$	3/2→ 5/2	4478.7961	4478.7950	1.1
	3/2→ 3/2	4465.2816	4465.2811	0.5
	3/2→ 1/2	4489.6166	4489.6181	−1.5
$1_{01} \rightarrow 2_{02}$	1/2→ 1/2	8951.3608	8951.3658	−5.0
	1/2→ 3/2	8937.8544	8937.8501	4.3
	3/2→ 3/2	8962.1960	8962.1983	−2.3
	5/2→ 5/2	8939.0123	8939.0135	1.2
	5/2→ 7/2	8952.5272	8952.5274	−0.2
$1_{10} \rightarrow 2_{11}$	1/2→ 1/2	9104.6107	9104.6085	2.2
	1/2→ 3/2	9097.8258	9097.8271	−1.3
	3/2→ 3/2	9085.6819	9085.6825	−0.6
	3/2→ 5/2	9080.8378	9080.8412	−3.4
	5/2→ 5/2	9087.5846	9087.5857	−1.1
	5/2→ 7/2	9094.3516	9094.3473	4.3
$1_{11} \rightarrow 2_{12}$	1/2→ 1/2	8824.2393	8824.2392	0.1
	1/2→ 3/2	8817.4834	8817.4841	−0.7
	3/2→ 3/2	8805.2923	8805.2922	0.1
	3/2→ 5/2	8800.4692	8800.4697	−0.5
	5/2→ 5/2	8807.2384	8807.2404	−2.0
	5/2→ 7/2	8813.9787	8813.9757	3.0
$2_{02} \rightarrow 3_{03}$	1/2→ 3/2 3/2→ 5/2	13422.3305	13422.3297	0.8
	5/2→ 7/2 7/2→ 9/2	13425.6856	13425.6840	1.6
	7/2→ 7/2	13412.1650	13412.1674	−2.4
$2_{11} \rightarrow 3_{12}$	1/2→ 3/2	13637.0844	13637.0867	−2.3
	3/2→ 5/2	13633.7073	13633.7128	−5.5
	5/2→ 7/2	13633.8169	13633.8119	5.0
	7/2→ 9/2	13637.1998	13637.1970	2.8
$2_{12} \rightarrow 3_{13}$	1/2→ 3/2	13216.5827	13216.5871	−4.4
	3/2→ 5/2	13213.2141	13213.2132	0.9
	5/2→ 7/2	13213.3073	13213.3058	1.5
	7/2→ 9/2	13216.6928	13216.6908	2.0

RESULTS

Spectra

Strong spectra exhibiting nuclear quadrupole multiplets indicative of the presence of a single chlorine nucleus ($I = \frac{3}{2}$) were readily observed for all three isotopes of the ethylene–HCl dimer. The $J = 0 \rightarrow 1$, $J = 1 \rightarrow 2$, and $J = 2 \rightarrow 3$ rotational transitions were measured for the ethylene–$H^{35}Cl$ and ethylene–$H^{37}Cl$ isotopic species and the $J = 1 \rightarrow 2$ and $J = 2 \rightarrow 3$ transitions were measured for the ethylene–$D^{35}Cl$ isotopic species. The ethylene–$H^{37}Cl$ spectrum was measured satisfactorily in natural abundance. The ethylene–DCl spectrum manifested extra splitting attributable to the deuterium nucleus ($I = 1$) which has a nuclear quadrupole moment. This extra splitting could be neglected with only a small loss in accuracy as the strongest components were shifted only slightly from the zero deuterium quadrupole frequencies.

The $K_{-1} = 2$, R-branch transitions were not measured. The rotational levels with $K_{-1} = 2$ are ~3 cm^{-1} higher in energy than the $K_{-1} = 0$ energy levels and thus are not sufficiently populated at the estimated ~4 K temperature of the gas.

Determination of molecular constants

The hyperfine components for the $J = 0 \rightarrow 1$, $J = 1 \rightarrow 2$, and $J = 2 \rightarrow 3$ rotational transitions for the ethylene–$H^{35}Cl$, ethylene–$H^{37}Cl$, and ethylene–$D^{35}Cl$ isotopic species are listed in Tables I, II, and III, respectively. The data in Tables I–III was reduced by the following two-step process. First, observed frequencies were corrected for second order quadrupole effects in the symmetric top basis. This is done with available tables[11] where a tabulated result for the corresponding symmetric top limit transition is multiplied by an approximate value for $2\chi_{aa}^2/(B+C)\times 10^{-3}$. Due to the estimated accuracy of the measurements of ~3 kHz, second order effects, where the nuclear quadrupole interaction is treated as a perturbation to the pure rotational Hamiltonian, are significant and range from 0–20 kHz. The two independent nuclear quadrupole coupling constants χ_{aa} and χ_{bb}, and the zero-quadrupole rotational frequencies ν_0, were then related to the observed quadrupole components ν_{ob} by the

TABLE II. Observed and calculated transition frequencies for C_2H_4–$H^{37}Cl$ (experimental uncertainty is estimated to be 3 kHz).

Rotational transition	$F \rightarrow F'$	Observed (MHz)	Calculated (MHz)	Difference (kHz)
$0_{00} \rightarrow 1_{01}$	3/2 → 1/2	4385.0300	4385.0329	−2.9
	3/2 → 3/2	4365.8447	4365.8450	−0.3
	3/2 → 5/2	4376.5016	4376.4983	3.3
$1_{01} \rightarrow 2_{02}$	1/2 → 1/2	8747.9889	8747.9891	−0.2
	3/2 → 3/2	8756.5305	8756.5331	−2.6
	3/2 → 5/2 5/2 → 7/2	8748.9083	8748.9055	2.8
$1_{10} \rightarrow 2_{11}$	1/2 → 3/2	8886.7284	8886.7264	2.0
	3/2 → 5/2	8873.3402	8873.3448	−4.6
	5/2 → 7/2	8883.9927	9883.9902	2.5
$1_{11} \rightarrow 2_{12}$	1/2 → 3/2	8618.9431	8618.9420	1.1
	5/2 → 7/2	8616.1801	8616.1822	−1.1
$2_{02} \rightarrow 3_{03}$	1/2 → 3/2 3/2 → 5/2	13118.0068	13118.0046	2.2
	5/2 → 7/2 7/2 → 9/2	13120.6485	13120.6507	−2.2
$2_{11} \rightarrow 3_{12}$	3/2 → 5/2	13319.7041	13319.7050	−0.9
	5/2 → 7/2	13319.7880	13319.7855	2.5
	7/2 → 9/2	13322.4537	13322.4552	−1.6
$2_{12} \rightarrow 3_{13}$	3/2 → 5/2	12918.0501	12918.0482	2.9
	5/2 → 7/2	12918.1172	12918.1180	−0.8
	7/2 → 9/2	12920.7883	12920.7904	−2.1

expression

$$\nu_{ob} - \Delta_{2nd} = C_a \chi_{aa} + C_b \chi_{bb} + \nu_0 , \quad (1)$$

where χ_{aa} and χ_{bb} are the Cl nuclear quadrupole coupling constants along the a and b principal axes, Δ_{2nd} is the second order nuclear quadrupole correction, and C_a and C_b are given by

$$C_a = \frac{1}{h}\left[f' \frac{2J'+3}{J'}(\alpha'^2_{az} - \alpha'^2_{cz}) - f \frac{2J+3}{J}(\alpha^2_{az} - \alpha^2_{cz})\right], \quad (2)$$

TABLE III. Observed and calculated transition frequencies for C_2H_4–$D^{35}Cl$ (experimental uncertainty is estimated to be 3 kHz).

Rotational transition	$F \rightarrow F'$	Observed (MHz)	Calculated (MHz)	Difference (kHz)
$1_{01} \rightarrow 2_{02}$	1/2 → 1/2	8968.0483	8968.0492	−0.9
	1/2 → 3/2	8953.9774	8953.9700	7.4
	3/2 → 3/2	8979.3296	8979.3266	3.0
	3/2 → 5/2 5/2 → 7/2	8969.2556	8969.2522	3.4
	5/2 → 5/2	8955.1791	8955.1807	−1.6
$1_{10} \rightarrow 2_{11}$	3/2 → 3/2	9102.4707	9102.4764	−5.7
	3/2 → 5/2	9097.4381	9097.4338	4.3
	5/2 → 7/2	9111.5049	9111.5034	1.5
$2_{02} \rightarrow 3_{03}$	1/2 → 3/2 3/2 → 5/2	13447.2278	13447.2388	−11.0
	5/2 → 7/2 7/2 → 9/2	13450.7417	13450.7327	9.0
	7/2 → 7/2	13436.6545	13436.6525	2.0
$2_{11} \rightarrow 3_{12}$	1/2 → 3/2	13662.6811	13662.6769	4.2
	3/2 → 5/2	13659.1621	13659.1639	−1.8
	5/2 → 7/2	13659.2623	13659.2671	−4.8
	7/2 → 9/2	13662.7972	13662.7930	4.2
$2_{12} \rightarrow 3_{13}$	3/2 → 5/2	13237.8036	13237.8096	−6.0
	5/2 → 7/2	13237.9065	13237.9062	0.3
	7/2 → 9/2	13241.4378	13241.4321	5.7

$$C_b = \frac{1}{h}\left[f' \frac{2J'+3}{J'}(\alpha'^2_{bz} - \alpha'^2_{cz}) - f\frac{2J+3}{J}(\alpha^2_{bz} - \alpha^2_{cz})\right], \quad (3)$$

$$f = \frac{3/4C(C+1) - I(I+1)J(J+1)}{2I(2I-1)(2J-1)(2J+3)}, \quad (4)$$

$$C = F(F+1) - I(I+1) - J(J+1). \quad (5)$$

α_{gz} is the direction cosine between the z axis and the g principal axis averaged over the appropriate asymmetric top wave function. Using this equation and applying the least-squares method to the observed frequencies in Tables I–III leads to the zero-quadrupole rotational frequencies in Table IV and the nuclear quadrupole coupling constants in Table V.

The results in Table IV were fit as described below with centrifugal distortion being treated in the symmetric top limit. This is justified by the near prolate value of κ and the limited number of transitions in the range of our spectrometer. Though exact analysis would employ nine τ distortion constants, the frequencies of only seven zero-quadrupole rotational transitions, all of which are $\Delta K = 0$, R branch, μ_a dipole type are presently available precluding this exact treatment. In the symmetric top limit, the centrifugal distortion contribution to each transition is given by

$$-4D_J(J+1)^3 - (2J+1)K^2_{-1}D_{JK}, \quad (6)$$

where

$$D_J = (-\hbar^4/4)\tau_{xxxx}, \quad (7)$$

$$D_{JK} = -2D_J - (\hbar^4/2)(\tau_{xxzz} + 2\tau_{xzxz}). \quad (8)$$

This follows from the Kivelson–Wilson treatment if we assume $K^n_{-1} \cong \langle P^n_z \rangle$ and if terms involving R_5, R_6, and δ_J can be neglected where[12]

$$R_5 = -\tfrac{1}{32}[\tau_{xxxx} - \tau_{yyyy} - 2(\tau_{xxzz} + 2\tau_{xzxz}) + 2(\tau_{yyzz} + 2\tau_{yzyz})]\hbar^4,$$

$$R_6 = \tfrac{1}{64}[\tau_{xxxx} + \tau_{yyyy} - 2(\tau_{xxyy} + 2\tau_{xyxy})]\hbar^4,$$

$$\delta_J = -\tfrac{1}{16}[\tau_{xxxx} - \tau_{yyyy}]\hbar^4. \quad (9)$$

TABLE IV. Observed and calculated unperturbed (zero quadrupole) center frequencies for three isotopes of the ethylene–HCl dimer.

Isotope	Transition	Observed (MHz)	Calculated (MHz)	Difference (kHz)
C_2H_4–$H^{35}Cl$	$0_{00} \leftarrow 1_{01}$	4476.0854	4476.0852	0.2
	$1_{01} \leftarrow 2_{02}$	8951.3661	8951.3663	−0.2
	$1_{10} \leftarrow 2_{11}$	9091.0579	9091.0470	10.9
	$1_{11} \leftarrow 2_{12}$	8810.6886	8810.6995	−10.9
	$2_{02} \leftarrow 3_{03}$	13425.0391	13425.0391	0.0
	$2_{11} \leftarrow 3_{12}$	13635.7455	13635.7532	−7.2
	$2_{12} \leftarrow 3_{13}$	13215.2407	13215.2334	7.3
C_2H_4–$H^{37}Cl$	$0_{00} \leftarrow 1_{01}$	4374.3609	4374.3622	−1.4
	$1_{01} \leftarrow 2_{02}$	8747.9894	8747.9883	1.1
	$1_{10} \leftarrow 2_{11}$	8881.3948	8881.3854	9.3
	$1_{11} \leftarrow 2_{12}$	8613.5894	8613.5987	−9.3
	$2_{02} \leftarrow 3_{03}$	13120.1420	13120.1423	−0.3
	$2_{11} \leftarrow 3_{12}$	13321.3101	13321.3163	−6.2
	$2_{12} \leftarrow 3_{13}$	12919.6441	12919.6379	6.2
C_2H_4–$D^{35}Cl$	$1_{01} \leftarrow 2_{02}$	8968.0494	8968.0489	0.5
	$1_{10} \leftarrow 2_{11}$	9108.0772	9108.0640	13.2
	$1_{11} \leftarrow 2_{12}$	8827.1314	8827.1446	−13.2
	$2_{02} \leftarrow 3_{03}$	13450.0610	13450.0611	−0.1
	$2_{11} \leftarrow 3_{12}$	13661.2812	13661.2900	−8.8
	$2_{12} \leftarrow 3_{13}$	13239.9216	13239.9128	8.8

TABLE V. Rotational constants, centrifugal distortion constants, and nuclear quadrupole coupling constants for three isotopes of the ethylene–HCl dimer.

	C_2H_4–$H^{35}Cl$	C_2H_4–$H^{37}Cl$	C_2H_4–$D^{35}Cl$
A(MHz)	25457(349)	25618(335)	25312(415)
B(MHz)	2308.143(3)	2254.141(3)	2312.457(4)
C(MHz)	2167.970(3)	2120.248(3)	2171.997(4)
D_J(kHz)	7.2(2)	6.7(2)	6.7(3)
D_{JK}(kHz)	282(5)	268(4)	272(6)
χ^{Cl}_{aa}(MHz)	−54.076(4)	−42.633(7)	−56.331(14)
χ^{Cl}_{bb}(MHz)	27.091(6)	21.399(13)	28.218(17)
χ^{Cl}_{cc}(MHz)	26.985(10)	21.235(19)	28.113(31)

R_5, R_6, and δ_J are clearly equal to 0 for a true symmetric top and the terms involving these quantities are expected to make minor contributions to centrifugal distortion for the transitions considered here. Also, since $\Delta K_{-1} = 0$, D_K need not be considered as its coefficient will always be 0 in the above approximation. This intuitively correct treatment was tested for accuracy with data for a molecule with a similar κ (vinyl bromide), where D_J and D_{JK} were calculated exactly from the τ's which were in turn calculated from a large number of different μ_a and μ_b transitions. Comparison of the exact D_J and D_{JK} with those obtained through our symmetric top limit analysis showed no difference outside of experimental error.

Using this symmetric top centrifugal distortion analysis, the zero-quadrupole rotational frequencies were fit in the following iterative fashion. Approximate guesses are made for A, B, and C. Next, rigid rotor frequencies are calculated by evaluating the matrix representation in the symmetric top basis for the rigid rotor, asymmetric top Hamiltonian

$$H = J^2_A\frac{2\pi A}{\hbar} + J^2_B\frac{2\pi B}{\hbar} + J^2_C\frac{2\pi C}{\hbar}. \quad (12)$$

The matrix is then diagonalized to give the rigid rotor asymmetric energy levels and subsequent asymmetric transition frequencies. Next, the following equation may be used iteratively to improve the values of A, B, and C and to obtain values for D_J and D_{JK}:

$$\Delta\nu = \nu_{ob} - \nu^{RR}_0 = \left(\frac{\partial\nu^{RR}}{\partial A}\right)_{B,C}\Delta A + \left(\frac{\partial\nu^{RR}}{\partial B}\right)_{A,C}\Delta B + \left(\frac{\partial\nu^{RR}}{\partial C}\right)_{A,B} - D_J 4(J+1)^3 - D_{JK}2(J+1)K^2_{-1}. \quad (13)$$

Here ν^{RR}_0 is the rigid rotor frequency obtained from the gradually improved values of A, B, and C $(\partial\nu^{RR}/\partial G_1)_{G_2,G_3}$ $(G_i = A, B, C)$ is a numerical derivative which may easily be evaluated, and ΔG is an unknown which is solved for by applying the least squares procedure and is then added to the rotational constant G to improve its accuracy each cycle. The final values of A, B, C, D_J, and D_{JK} are given in Table V. The residues in Table IV reflect the slight error introduced when not using the terms which are defined in Eq. (9).

The edge to chlorine distances are given in Table VI (see Fig. 1). Due to zero-point vibrational effects, a slightly different distance is obtained by fitting B and C (for example 3.721 vs 3.727 Å for ethylene–$H^{35}Cl$).

TABLE VI. Planar moments for three isotopic species of the ethylene–HCl dimer and for ethylene.

	Ethylene–$H^{35}Cl$	Ethylene–$H^{37}Cl$	Ethylene–$D^{35}Cl$	Ethylene
P_a (amu Å^2)[a]	216	221	216	16.85
P_b (amu Å^2)[b]	17.0	16.9	17.1	3.505
P_c (amu Å^2)[c]	2.85	2.78	2.92	−0.013

[a] $P_a = \frac{1}{2}(-I_{aa}+I_{bb}+I_{cc})$. [b] $P_b = \frac{1}{2}(-I_{bb}+I_{aa}+I_{cc})$. [c] $P_c = \frac{1}{2}(-I_{cc}+I_{aa}+I_{bb})$.

Thus the distance given in Table VI is an average obtained using

$$\sum_i m_i(a_i^2+c_i^2) = I_{bb} , \tag{14}$$

$$\sum_i m_i(a_i^2+b_i^2) = I_{cc} , \tag{15}$$

and utilizing the center of mass condition

$$\sum_i m_i a_i = 0 . \tag{16}$$

Structure

The following conclusions can be derived unambiguously from the spectra: the dimer is nonplanar with the HCl molecule perpendicular to the plane of the ethylene molecule. The hydrogen atom is between the chlorine atom and ethylene pointing midway between the carbon atoms. Also, the HCl molecule lies on the C_2 symmetry axis of the dimer which is additionally the a principal axis.

The nonplanarity of the complex is best revealed by the P_c of the dimer which is listed for all three isotopes in Table VI. An estimate based on a rigid nonplanar C_{2v} model gave $P_c = 3.45$ amu Å^2. Although calculation for the rigid planar C_{2v} model gives $P_c = 0$ by necessity, a slightly larger value would be observed in a real planar molecule due to zero-point vibrational effects. Values of P_c between 1 and 1.5 amu Å^2 have been observed for van der Waals complexes of argon with CO_2 and ClCN.[13,14]

Further evidence for the nonplanarity of the dimer follows from consideration of the rotational constants. From an infrared study it has been determined that the B and C rotational constants of ethylene are 29 990 and 24 860 MHz, respectively.[15] The c principal axis of ethylene is perpendicular to the plane of the ethylene molecule while the b principal axis is in the plane of the ethylene molecule and perpendicular to the carbon–carbon bonding axis. Thus the c principal axis of ethylene becomes the a principal axis in the C_{2v} nonplanar model of the dimer whereas if the dimer were planar, with HCl in the plane of the ethylene molecule perpendicular to the carbon–carbon axis, the b principal axis of ethylene would become the a principal axis of the dimer. It is clear that these are the likely possibilities. Thus the fact that the A rotational constant of the dimer is so close to the C rotational constant of free ethylene and keeping in mind that HCl is presumed to be on the a principal axis on average for reasons to be discussed shortly and thus does not contribute to the moment of inertia about the a principal axis, it is clear that the nonplanar model described above is supported. If the planar model was the correct one, we would expect instead for the B rotational constant of free ethylene to be approximately equal to the A rotational constant of the dimer. This is clearly not the case.

One further piece of evidence for the nonplanar C_{2v} model involves the values of the planar moments P_a, P_b, and P_c for the dimer and for free ethylene, where

$$P_a = \tfrac{1}{2}(-I_{aa}+I_{bb}+I_{cc}) = \sum_i m_i a_i^2 , \tag{17}$$

$$P_b = \tfrac{1}{2}(-I_{bb}+I_{aa}+I_{cc}) = \sum_i m_i b_i^2 , \tag{18}$$

$$P_c = \tfrac{1}{2}(-I_{cc}+I_{aa}+I_{bb}) = \sum_i m_i c_i^2 . \tag{19}$$

Figure 2 shows the orientation of the principal axes of the dimer with respect to the ethylene subunit and the principal axis system of free ethylene with respect to the molecule. Table VI gives values of P_a, P_b, and P_c for all three isotopes of the dimer and for free ethylene. Since in going from the free ethylene to the dimer the a and b principal axes of the free ethylene molecule become the b and c principal axes of the dimer, respec-

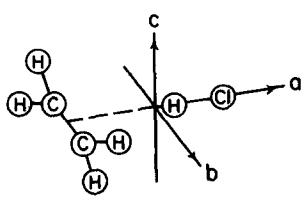

FIG. 1. Molecular geometry and identification of the principal axes in the ethylene–HCl dimer.

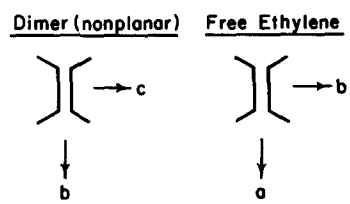

FIG. 2. Orientation of the principal axes with respect to ethylene in free ethylene and the ethylene–HCl dimer.

tively, we would expect a strong correlation of P_a and P_b[16] of the ethylene molecule with the P_b and P_c values, respectively, of the dimer, with any difference being due to the vibrational modes created upon complexation. It is clear from the table that nonplanarity is once again firmly established as in the planar model $P_c^{\text{dimer}} \ll P_b^{C_2H_4}$.

As has been mentioned, HCl lies on the a principal axis. This is quite clear from the A rotational constants given in Table V. The conclusion to be drawn from these values is that within experimental error the moment of inertia about the a principal axis does not change upon isotopic substitution of the chlorine or the hydrogen. This can only be true if the HCl subunit lies on the a principal axis. Also it is clear from the rotational constants that the hydrogen atom is between the chlorine atom and ethylene. This is evident from the small effect deuteration has on the moments of inertia about the b and c principal axes as compared to the dramatic change on ^{37}Cl substitution. This of course follows from the proximity of the hydrogen atom to the center of mass.

Lastly, regarding structure, it will be mentioned that the effects of C_{2V} symmetry on line intensities were observed in a qualitative way in that the intensities of $K_{-1}=0$ lines seemed enhanced over the normal line strength factor. This is consistent with the nuclear spin statistics appropriate for a dimer with two sets of fermions (hydrogen nuclei) that exchange through a C_2 symmetry operation. Since both pairs of hydrogen nuclei obey Fermi–Dirac statistics, a C_2 symmetry operation leaves the overall wave function unchanged. Therefore the overall wave function ψ is symmetric where

$$\psi = \psi_e \psi_v \psi_r \psi_n \,, \tag{20}$$

and ψ_e, ψ_v, ψ_r, and ψ_n are the electronic, vibrational, rotational, and nuclear wave functions, respectively. As the dimer is in its vibronic ground state, the parity and consequent degeneracy of ψ_n is determined by the parity of the rotational wave function. For the near prolate asymmetric top, all K_{-1} even levels will have symmetric rotational wave functions and all K_{-1} odd levels will have antisymmetric rotational wave functions with respect to a C_2 symmetry operation about the a principal axis. As the degeneracies of corresponding nuclear wave functions are given by

$$\eta_{sym} = \frac{1}{2}\left[\prod_{i=1}^{n}(2I_i+1)\right]\left[\prod_{i=1}^{n}(2I_i+1)+1\right] \,, \tag{21}$$

$$\eta_{antisym} = \frac{1}{2}\left[\prod_{i=1}^{n}(2I_i+1)\right]\left[\prod_{i=1}^{n}(2I_i+1)-1\right] \,, \tag{22}$$

there will be a 5/3 ratio over the normal line strength factor favoring J_{eo} and J_{ee} levels.

Internal dynamics and binding

The attractive interaction between HCl and ethylene is presumed to be that of a hydrogen bond with the electrophilic hydrogen atom of HCl forming a bond with the nucleophilic π electron density of ethylene. Because of this presumption it is expected that the molecular constants describing both the binding of HCl to ethylene and the motion of the hydrogen in its excursions from its equilibrium position on the a principal axis are likely to reflect this. Special attention will first be given to this later point.

TABLE VII. Molecular multipole moments of ethylene.

Qm_{zz} (esu cm^2)	1.979×10^{-26} [17]
Φ_{zzzz} (esu cm^4)	-6.596×10^{-42} [18]

The relation of the nuclear quadrupole coupling constant of chlorine in free HCl to that of chlorine in the dimer is given by

$$\chi_{gg} = \chi^0_{HCl}\left\langle\frac{3\alpha^2_{HCl,g}-1}{2}\right\rangle \,, \quad g=a,b,c, \tag{23}$$

where χ^0_{HCl} is the free HCl coupling constant taken from the literature,[17] and χ_{gg} is the nuclear quadrupole coupling constant of chlorine in the complex along the g principal axis of the dimer, and $\alpha_{HCl,g}$ is the direction cosine between the axis of the HCl bond and the g principal axis of the dimer. The averaging is over the zero point vibrational motion of the dimer which involves primarily the van der Waals bending modes. An assumption is made here that the electric field gradient at the chlorine is unchanged upon dimer formation and thus only a geometric effect is being considered here. Before proceeding, this assumption can be tested in an approximate way. Approximation of the potential with a multipole expansion has proved revealing with rare gas, hydrogen halide complexes. Under this approximation the potential at a given point (r,θ) due to the presence of an uncharged molecule attributed with various multipole moments is given by

$$V(r,\theta) = \frac{\mu P_1(\cos\theta)}{r^2} + \frac{Q_m P_2(\cos\theta)}{r^3} + \frac{\Omega P_3(\cos\theta)}{r^4} + \frac{\phi P_4(\cos\theta)}{r^5} \cdots \tag{24}$$

This expansion neglects the near isotropic repulsive potential. By noting that only even terms will be nonzero for ethylene and truncating after the hexadecapole term we obtain

$$V(r,\theta) \cong \frac{Q_m P_2(\cos\theta)}{r^3} + \frac{\phi P_4(\cos\theta)}{r^5} \,, \tag{25}$$

where Q_m and ϕ are the quadrupole and hexadecapole moments, respectively, for ethylene from the literature[18,19] and listed in Table VII. By twice differentiating and changing sign the electric field gradient at chlorine can now be approximated by

$$V_{aa}(r,\theta) \cong \frac{-12Q_m P_2(\cos\theta)}{r^5} - \frac{30\phi P_4(\cos\theta)}{r^7} \,, \tag{26}$$

where the distances are along the a principal axis and the angle θ is between the a principal axis and the symmetry axis of ethylene. This contribution to the electric field gradient will however be enhanced by the Sternheimer shielding phenomenon.[20] Thus there will be another contribution besides that given in Eq. (25) which comes about from ethylene inducing a quadrupole moment in the electronic distribution surrounding the chlorine nucleus

TABLE VIII. Some molecular constants of three isotopes of the ethylene–HCl dimer.

	C_2H_4–H ^{35}Cl	C_2H_4–H ^{37}Cl	C_2H_4–D ^{35}Cl
k_s (mdyn Å^{-1})	0.066	0.066	0.070
ν_s (cm^{-1})	84.3	83.3	86.3
γ (degrees)	21.43	21.42	19.49
θ_b (degrees)	15.46	15.39	13.99
θ_c (degrees)	15.57	15.61	14.11
r (Å)	3.724	3.724	3.719
ϵ (cm^{-1})	627	627	663

which in turn induces an electric field gradient at the chlorine nucleus. Thus the total contribution to the electric field gradient at the chlorine nucleus due to the presence of the ethylene molecule is given by

$$q_{aa}^{\text{total}} = q_{aa}^{\text{ext}} + q_{aa}^{\text{ind}} . \tag{27}$$

If we define a constant of the chlorine electronic distribution γ_∞ such that

$$\gamma_\infty = -q_{aa}^{\text{induced}}/q_{aa}^{\text{ext}} , \tag{28}$$

then we may write

$$q_{aa}^{\text{total}} = q_{aa}^{\text{ext}}(1-\gamma_\infty) . \tag{29}$$

Good values of γ_∞ are obtainable for Cl^-, but not for atomic chlorine though they are expected to be around -10 to -20. The degree of ionization in HCl of chlorine can be estimated by noticing that in NaCl where chlorine is totally ionized the nuclear quadrupole coupling constant of chlorine is about 0 while that of atomic chlorine is around 107 MHz. Since in HCl, the nuclear quadrupole coupling constant is -67.618, we would estimate that chlorine in HCl is about 37% ionized. Pauling's estimate puts it lower at ~ 17%.[21] Using the value of γ_∞ for Cl^- of -83.5,[22] we might estimate γ_∞ to be ~ -30. Thus the total contribution of electric field gradient at the chlorine nucleus due to the presence of the ethylene molecule would be expected to be $\sim 0.75\times10^{14}$ esu cm^{-3}. To see how this compares to the measured electric field gradient at chlorine in the dimer we may use the measured value of χ_{aa} for the dimer and the expression

$$\chi_{aa} = (-|e|q_{aa}Q/h) , \tag{30}$$

and the value -0.085×10^{-24} cm^2 for the quadrupole moment of chlorine[11] to obtain $q_{aa}^{\text{measured}} = -87.82\times10^{14}$ esu cm^{-3}. Thus the electrostatic properties of the ethylene molecule are accounting for less than 1% of the electric field gradient at the Cl nucleus and thus the change in χ_{aa} upon dimer formation for chlorine can be explained almost entirely as arising from geometric effects described by Eq. (23).

If we let $g = a$ in Eq. (23) then $\alpha_{\text{HCl}g}$ is the cosine of the instantaneous angle between the HCl bond axis with the a principal axis of the dimer. The operationally defined angle γ obtained from Eq. (23) is thus a relative measure of how constrained the hydrogen is in its zero point vibrational exclusions from the a principal axis. This angle is listed in Table VIII for all three isotopes. The magnitude of the angle obtained is consistent with the notion of the complex being hydrogen bonded. This point will be discussed later. In the present system the motion of the electrophilic hydrogen is perhaps better described by angles which reflect its motion from the a principal axis in the ab plane and the ac plane. This can be carried out by performing two simultaneous rotations $\mathbf{R}_1(\alpha)$ and $\mathbf{R}_2(\beta)$, on the nuclear quadrupole coupling constant tensor of free HCl, which is symmetric in its principal axis system, to bring the tensor into the principal axis system of the dimer. Thus

$$\mathbf{U}\begin{pmatrix} \chi^0 & 0 & 0 \\ 0 & -\frac{\chi^0}{2} & 0 \\ 0 & 0 & -\frac{\chi^0}{2} \end{pmatrix}\mathbf{U}^{-1} = \mathbf{X}^{\text{dimer}} , \tag{31}$$

where

$$\mathbf{U} = \mathbf{R}_2(\beta)\mathbf{R}_1(\alpha) . \tag{32}$$

The ab plane and ac plane bending angles θ_b and θ_c are thus related to the Euler angles α and β by simple trigonometric relations that depend upon how the rotations are defined. The resulting expression for θ_b and θ_c gives

$$\theta_b = \arccos\left[\frac{\chi_{aa}+\chi^0_{\text{HCl}}/2}{\chi_{aa}+\chi_{bb}+\chi^0_{\text{HCl}}}\right]^{1/2} , \tag{33}$$

$$\theta_c = \arccos\left[\frac{\chi_{aa}+\chi^0_{\text{HCl}}/2}{\chi_{aa}+\chi_{cc}+\chi^0_{\text{HCl}}}\right]^{1/2} . \tag{34}$$

Alternately, these expressions can be derived by noting that

$$\cos\theta_b = \alpha_{\text{HCl}a}/\sqrt{\alpha^2_{\text{HCl}a}+\alpha^2_{\text{HCl}b}} , \tag{35}$$

$$\cos\theta_c = \alpha_{\text{HCl}a}/\sqrt{\alpha^2_{\text{HCl}a}+\alpha^2_{\text{HCl}c}} , \tag{36}$$

and utilizing Eq. (23). The values for θ_b and θ_c are given in Table VIII for all three isotopic species. It is apparent from these values that the motion of the hydrogen is at best slightly less constrained in the direction perpendicular to the carbon–carbon bonding axis as compared with the direction along the carbon–carbon bonding axis and thus generally speaking the potential in which the hydrogen atom moves is very nearly isotropic.

To get a relative measure of how tightly bound the complex is as compared to other hydrogen-bound and non-hydrogen-bound systems it is helpful to use a simple diatomic model which makes use of the fact that the frequencies of the stretching and bending modes of the hydrogen bond are in general much lower than those of the monomers. This is especially useful for the rare gas, hydrogen halide complexes and even the hydrogen-bound systems of diatomics. In the present case its validity is somewhat diminished as the natural frequencies of some of the bending modes of ethylene begin to approach the hydrogen bond stretching frequency of ~ 84 cm^{-1} calculated using

$$\nu_s = (4B_0^3/D_J)^{1/2} , \tag{37}$$

where

$$\overline{B}_0 = (B+C/2) , \tag{38}$$

thus presenting more serious coupling complications than in these simple complexes. Keeping in mind that it

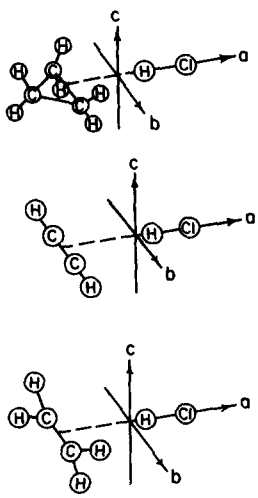

FIG. 3. Molecular geometry and identification of the principal axes in three similar hydrogen-bound dimers.

is at best an approximation, k_s values are listed in Table VIII for all three isotopes using the diatomic harmonic oscillator relationship

$$\nu_s = 1/2\pi(k_s/\mu_s)^{1/2} , \tag{39}$$

and

$$\mu_s = M_{HCl}M_{C_2H_4}/M_{HCl} + M_{C_2H_4} . \tag{40}$$

Similarly, keeping with the diatomic model, we can describe the radial potential governing the hydrogen bond interaction with a Lennard-Jones 6/12 potential given by

$$V(R) = \epsilon[(R_e/R)^{12} - 2(R_e/R)^6] , \tag{41}$$

TABLE IX. Comparison of k_s and ϵ for various hydrogen-bound and nonhydrogen-bound dimers.

		k_s (mdyn Å^{-1})	ϵ (cm^{-1})
Hydrogen-bound	C_2H_4–HCl	0.066	627
	C_2H_2–HCl[a]	0.069	643
	OC–HCl[b]	0.045	569
	HCN–HCN[c]	0.110	1540
	HF–HCl[d]	0.057	451
	OC–HBr[e]	0.0113	469
van der Waals	KrHBr[f]	0.0192	247
	ArHBr[g]	0.0166	206
	KrHCl	0.0156	180

[a]Reference 1.
[b]P. D. Soper, A. C. Legon, and W. H. Flygare, J. Chem. Phys. 74, 2138 (1981).
[c]L. W. Buxton, E. J. Campbell, and W. H. Flygare, Chem. Phys. 54, 173 (1981).
[d]K. C. Janda, J. M. Steed, S. E. Novick, and W. Klemperer, J. Chem. Phys. 67, 5162 (1977).
[e]M. R. Keenan, T. K. Minton, A. C. Legon, T. J. Balle, and W. H. Flygare, Proc. Natl. Acad. Sci. USA 77, 5583 (1980).
[f]M. R. Keenan, E. J. Campbell, T. J. Balle, L. W. Buxton, T. K. Minton, P. D. Soper, and W. H. Flygare, J. Chem. Phys. 72, 3070 (1980).
[g]T. J. Balle, E. J. Campbell, M. R. Keenan, and W. H. Flygare, J. Chem. Phys. 72, 922 (1980).

TABLE X. Comparison of γ for various hydrogen-bound and nonhydrogen-bound dimers.

		γ (degrees)
Hydrogen-bound	C_2H_4–HCl	21
	HF–HCl[a]	23
	C_2H_2–HCl[b]	21
	OC–HBr[c]	23
van der Waals	ArDF[d]	32
	KrHCl[e]	38
	XeHCl[e]	35

[a]Reference (d) in Table IX.
[b]Reference 1.
[c]E. J. Campbell, L. W. Buxton, M. R. Keenan, and W. H. Flygare, J. Chem. Phys. 74, 2133 (1981).
[d]M. B. Keenan, L. W. Buxton, E. J. Campbell, A. C. Legon, and W. H. Flygare, J. Chem. Phys. 74, 2133 (1981).

which can be expanded in a Taylor series about $R = R_e$ giving

$$V(R) = -\epsilon + \frac{36\epsilon}{R_e^2}(R - R_e)^2 - \frac{252\epsilon}{R_e^3}(R - R_e)^3 , \tag{42}$$

where ϵ is the well depth and R_e is the equilibrium intermolecular distance. We can therefore equate the coefficient of the quadratic term to one half the harmonic oscillator force constant. Thus, we have

$$\epsilon = (k_s R_e^2/7\ 2) \tag{43}$$

Values for ϵ for all three isotopes are listed in Table VIII where we have approximated R_e by using the observed distance between the centers of mass of the two monomers.

DISCUSSION

The rotational spectrum of the ethylene–HCl dimer is unambiguous both with regard to structure and to the nature of the bond. The structure is clearly determined to have HCl on average along the a principal axis, which is also the C_2 axis of the dimer, and perpendicular to the plane of the ethylene molecule thus making the complex nonplanar. The hydrogen atom is close to ethylene and participates in a hydrogen bond type interaction with the π electron density of the ethylene molecule.

The structure is not surprising especially in light of the discovery of the cyclopropane–HCl and acetylene–HCl dimers which have very similar structures and properties. All three dimers have HCl along the a principal axis perpendicular to a carbon–carbon bonding axis (see Fig. 3) and have values of χ_{aa} of ~ −54.4 MHz. The similarity of the ethylene–HCl and acetylene–HCl dimers is especially apparent in the edge to chlorine distances (3.72 vs 3.69 Å) and in the hydrogen bond force constants and well depth estimated from the diatomic model. These values are included in Table IX for acetylene–HCl and other hydrogen-bonded dimers and for the rare gas hydrogen halide complexes. It is clear from comparison that the ethylene–HCl dimer compares more closely to the hydrogen-bound category than the more traditional van der Waals molecules. This point is also brought out by comparison of the angle γ, oper-

ationally defined by Eq. 23 and where $g = a$, for various dimers. This angle is essentially a measure of how much the electrophilic hydrogen in these dimers is participating in the bonding process. For the hydrogen-bound dimers this angle is between 21° and 23° but in the traditional van der Waals molecules it is between 30° and 40° indicating that the hydrogen is virtually unconstrained in its motion about its average position. Table X compares this angle for the ethylene–HCl dimer with those for other hydrogen-bound systems. Once again the same conclusion is drawn.

ACKNOWLEDGMENT

The support of the National Science Foundation is gratefully acknowledged.

[1]A. C. Legon, P. D. Aldrich, and W. H. Flygare, J. Am. Chem. Soc. **102**, 7584 (1980).
[2]A. C. Legon, P. D. Aldrich, and W. H. Flygare, J. Am. Chem. Soc. (to be published).
[3]A. C. Legon, P. D. Aldrich, and W. H. Flygare, J. Chem. Phys. **75**, 625 (1981).
[4]E. L. Parlee and R. W. Taft, J. Am. Chem. Soc. **78**, 5807 (1956).
[5]M. J. S. Dewar, *The Molecular Orbital Theory of Organic Chemistry* (McGraw-Hill, New York, 1969).
[6]F. Badea, *Reaction Mechanisms in Organic Chemistry* (Abacas, Kent, England, 1977).
[7]T. J. Balle, E. J. Campbell, M. R. Keenan, and W. H. Flygare, J. Chem. Phys. **71**, 2723 (1979).
[8]T. J. Balle, E. J. Campbell, M. R. Keenan, and W. H. Flygare, J. Chem. Phys. **72**, 922 (1980).
[9]T. J. Balle and W. H. Flygare, Rev. Sci. Instrum. **52**, 33 (1981).
[10]E. J. Campbell, L. W. Buxton, T. J. Balle, M. R. Keenan, and W. H. Flygare, J. Chem. Phys. **74**, 829 (1981).
[11]C. H. Townes and A. L. Schawlow, *Microwave Spectroscopy* (Dover, New York, 1955).
[12]W. Gordy and R. Cook, *Microwave Molecular Spectra* (Interscience, New York, 1970).
[13]J. M. Steed, T. A. Dixon, and W. Klemperer, J. Chem. Phys. **70**, 4095 (1979).
[14]M. R. Keenan, D. Wozniak, and W. H. Flygare, J. Chem. Phys. **75**, 631 (1981).
[15]H. C. Allen and E. K. Plyer, J. Am. Chem. Soc. **80**, 2673 (1958).
[16]P_a and P_b values for free ethylene are calculated from values for A, B, and C given in G. Herzberg, *Molecular Spectra and Molecular Structure* (III), (Van Nostrand, New York, 1966).
[17]E. W. Kaiser, J. Chem. Phys. **53**, 1686 (1970).
[18]C. Hosticka, T. K. Bose, and J. S. Sochanski, J. Chem. Phys. **61**, 2575 (1974).
[19]R. D. Amos and J. H. Williams, Chem. Phys. Lett. **66**, 471 (1979).
[20]R. Sternheimer, Phys. Rev. **80**, 102 (1950); **84**, 244 (1951); **86**, 316 (1952); **95**, 736 (1954).
[21]L. Pauling, *The Chemical Bond* (Cornell University, Ithaca, 1967).
[22]F. D. Feiock and W. R. Johnson, Phys. Rev. **187**, 39 (1969).